J. Chem. Thermodynamics 131 (2019) 375–386

Contents lists available at ScienceDirect

J. Chem. Thermodynamics

journal homepage: www.elsevier.com/locate/jct

Solubility of U(VI) in chloride solutions. III. The stable oxides/hydroxides in $MgCl_2$ systems: Pitzer activity model for the system UO_2^{2+}–Na^+–K^+–Mg^{2+}–H^+–OH^-–Cl^-–H_2O(l)

Ezgi Yalçıntaş [a,b,*], Neşe Çevirim-Papaioannou [a], Xavier Gaona [a], David Fellhauer [a], Volker Neck [a], Marcus Altmaier [a,*]

[a] Institute for Nuclear Waste Disposal, Karlsruhe Institute of Technology, P.O. Box 3640, Karlsruhe, Germany
[b] Los Alamos National Laboratory, Carlsbad, NM, 88220, USA

ARTICLE INFO

Article history:
Received 5 October 2018
Received in revised form 16 October 2018
Accepted 18 October 2018
Available online 24 October 2018

Keywords:
Uranium(VI)
Hydrolysis
Solubility
NaCl
KCl
$MgCl_2$
Pitzer

ABSTRACT

We have developed new chemical, thermodynamic and activity models for the system UO_2^{2+}–Na^+–K^+–Mg^{2+}–H^+–OH^-–Cl^-–H_2O(l) within the Pitzer approach. The new thermodynamic model is based on previously reported data treated within the SIT approach for NaCl and KCl systems, as well as on new experimental data determined in this work for the $MgCl_2$ system.

The solubility of uranium(VI) was studied in 0.01–5.15 mol·kg$_w^{-1}$ $MgCl_2$ solutions at pH_m = 4.1–9.7 (with $pH_m = -\log [H^+]$). Experiments were performed under Ar atmosphere at T = (22 ± 2) °C. In all investigated systems, the solubility of U(VI) is controlled by metaschoepite, $UO_3{\cdot}2H_2O$(cr). In contrast to previously investigated NaCl and KCl systems, no ternary Mg–U(VI)–OH(s) solid phases formed in alkaline $MgCl_2$ solutions within the timeframe of this study (≤ 200 days). A very significant increase in the solubility (up to 3 $\log_{10}$-units) is observed in acidic to near-neutral pH_m conditions when increasing $MgCl_2$ concentration from 0.01 to 5.15 mol·kg$_w^{-1}$, which reflects the strong ion interaction processes taking place in concentrated $MgCl_2$ brines.

The solubility of $UO_3{\cdot}2H_2O$(cr) in the investigated NaCl, KCl and $MgCl_2$ solutions is well described with the solubility and hydrolysis constants recommended by Altmaier et al., (2017) and NEA–TDB, and a Pitzer activity model derived in the present work. The latter model considers experimental data reported in the present study and available in the literature for NaCl, KCl and $MgCl_2$ systems (solubility, potentiometric and spectroscopic data), in combination with well-stablished estimation methods and correlations with SIT coefficients.

Chemical, thermodynamic and Pitzer activity models provided in this work for the system UO_2^{2+}–Na^+–K^+–Mg^{2+}–H^+–OH^-–Cl^-–H_2O(l) accurately describe all evaluated datasets, and represent an adequate tool for the calculation of U(VI) solubility and aqueous speciation in a variety of geochemical conditions including concentrated brine systems of relevance in salt-based repositories for nuclear waste disposal.

Published by Elsevier Ltd.

1. Introduction

An accurate understanding of the solubility and speciation of U(VI) in dilute to concentrated salt systems is required in the Safety Assessment of repositories for the disposal of nuclear waste. Geochemical boundary conditions in the repository strongly depend on the type of host-rock formation (crystalline, clay, salt), backfill material and waste form. Na, Mg and K are abundant cations in different types of groundwater, but can be of particular relevance in the case of water intrusion into salt-rock formations. Rather high concentrations of Na and K (0.1–0.2 mol·dm^{-3}) are found in the pore waters of cement within its first degradation stage, until the soluble oxides Na_2O and K_2O are completely washed out [1,2]. Soluble Na and Mg salts are characteristic for rock salt environments and are for instance present in the Asse salt dome (Germany) [3]. In the context of the currently operating Waste Isolation Pilot Plant (WIPP) in Carlsbad (USA), aqueous systems with high ionic strength are expected to form in certain scenarios. The composition of these brines is mostly dominated

* Corresponding authors at: Los Alamos National Laboratory, Carlsbad, NM, 88220, USA (E. Yalçıntaş); Institute for Nuclear Waste Disposal, Karlsruhe Institute of Technology, P.O. Box 3640, Karlsruhe, Germany (M. Altmaier).
E-mail addresses: eyalcintas@lanl.gov (E. Yalçıntaş), marcus.altmaier@kit.edu (M. Altmaier).

https://doi.org/10.1016/j.jct.2018.10.019
0021-9614/Published by Elsevier Ltd.

by NaCl, $MgCl_2$ and KCl, with minor contributions of Ca^{2+}, HCO_3^- and Br^- ions [4]. The use of MgO as backfill material represents an additional alteration of the geochemical conditions, buffering the pH and reducing carbonate concentration by precipitation of $MgCO_3(s)$.

The chemical thermodynamics of U(VI) hydrolysis species and oxide/hydroxide solid phases forming in dilute to concentrated NaCl and KCl were recently investigated by Altmaier et al. (2017) [5] and Cevirim-Papaioannou et al. (2018) [6] in comprehensive studies. A summary of thermodynamic data derived with SIT reported in these publications is provided in Section 1.1, in connection with other thermodynamic studies available in the literature and with the current NEA–TDB thermodynamic selection. In contrast to NaCl and KCl systems, the solubility of U(VI) has not been investigated so far in dilute to concentrated $MgCl_2$ solutions, and there are no activity models available able to reliably calculate activity coefficients of U(VI) hydrolysis species in concentrated $MgCl_2$ brines. For all NaCl, KCl and $MgCl_2$ systems a comprehensive thermodynamic model using Pitzer for high ionic strength (I) conditions is missing.

In contrast to the reported formation of Na-, K-, and Ca-uranates in alkaline NaCl, KCl and $CaCl_2$ solutions [5–7], there is no experimental evidence so far reporting the formation of analogous Mg–uranate compounds in alkaline $MgCl_2$ solutions at room temperature. For instance, a $MgUO_4(cr)$ phase synthesized at $T \geq 1000$ K [8,9] is the only Mg-uranate compound currently selected in the OECD/Nuclear Energy Agency Thermochemical Database (NEA–TDB) [10]. Vochten et al. (1991) [11] synthesized $Mg[(UO_2)_6O_4(OH)_6]\cdot 10H_2O(cr)$ by equilibrating $UO_3\cdot 2H_2O(cr)$ in 0.5 mol·dm^{-3} $MgSO_4$ under mildly hydrothermal conditions (333 K) for two weeks, but the formation of analogous phases at ambient temperature conditions remains putative. In this context, the present study aims at a systematic experimental investigation of U(VI) solubility in dilute to concentrated $MgCl_2$ systems, complemented with solid phase characterization and aqueous speciation techniques.

Solubility data determined in this work is evaluated in combination with previous solubility and potentiometric studies in NaCl/KCl systems [5,6,12–14], and taking as anchoring point U(VI) solubility and hydrolysis constants summarized in [5]. The final goal is to derive a comprehensive chemical, thermodynamic and Pitzer activity model for the system UO_2^{2+}–Na^+–K^+–Mg^{2+}–H^+–OH^-–Cl^-–$H_2O(l)$ that can be implemented in thermodynamic databases, and accordingly used in geochemical calculations of relevance in the context of nuclear waste disposal.

1.1. Current chemical, thermodynamic and SIT activity models for the system UO_2^{2+}–Na^+–K^+–H^+–OH^-–Cl^-–$H_2O(l)$

Thermodynamic data for the solubility and hydrolysis of U(VI) in acidic to hyper-alkaline pH conditions was recently updated by Altmaier et al. (2017) [5]. The updated thermodynamic model using the SIT approach was based on new solubility experiments in dilute to concentrated NaCl systems, previously reported potentiometric studies [12–14], and taking as anchoring point thermodynamic data selected in the NEA–TDB for the hydrolysis species of U(VI) forming in acidic conditions [10]. Solubility data in alkaline NaCl solutions was used to derive $\log {}^*K^\circ_{s,0}\{0.5Na_2U_2O_7\cdot H_2O(cr)\}$ [15] and hydrolysis constants for the anionic species $UO_2(OH)_3^-$ and $UO_2(OH)_4^{2-}$. This SIT model was extended later by Cevirim-Papaioannou et al. (2017) [6] to near-neutral to hyperalkaline KCl systems, where the solid phases $K_2U_6O_{19}\cdot 11H_2O(cr)$ and $K_2U_2O_7\cdot 1.5H_2O(cr)$ were reported to control the solubility of U(VI). Tables 1 and 2 summarize the chemical, thermodynamic and SIT activity models reported in the literature and considered in this work as basis for the development of a Pitzer activity model for NaCl, KCl and $MgCl_2$ systems.

Table 2
SIT ion interaction coefficients (in kg·mol^{-1}) reported in the literature for UO_2^{2+} and U(VI) hydrolysis species in NaCl and KCl systems.

U(VI) species		SIT coefficients	
i	j	$\varepsilon(i,j)$	References
UO_2^{2+}	Cl^-	(0.21 ± 0.02)	[16]
UO_2OH^+	Cl^-	(0.10 ± 0.10)	[5]
$(UO_2)_2(OH)_2^{2+}$	Cl^-	(0.30 ± 0.06)	[5]
$(UO_2)_3(OH)_4^{2+}$	Cl^-	−(0.07 ± 0.17)	[5]
$(UO_2)_3(OH)_5^+$	Cl^-	(0.24 ± 0.15)	[5]
$(UO_2)_4(OH)_7^+$	Cl^-	(0.17 ± 0.18)	[5]
$UO_2(OH)_3^-$	Na^+	−(0.24 ± 0.09)	[5]
	K^+	−(0.24 ± 0.09)	[6]
$UO_2(OH)_4^{2-}$	Na^+	(0.01 ± 0.04)	[5]
	K^+	(0.03 ± 0.04)	[6]
$(UO_2)_3(OH)_7^-$	Na^+	−(0.24 ± 0.09)	[5]
	K^+	−(0.24 ± 0.09)	[6]
$UO_2(OH)_2(aq)$	Na^+, K^+, Cl^-	0	a

[a]By definition in SIT.

1.2. Pitzer activity model

The Pitzer activity model is widely acknowledged as one of the most accurate approaches for the determination of activity coefficients of single ions in mixed electrolyte systems at high ionic strength. Especially for concentrated salt brine solutions, the use of the Pitzer model is strongly recommended for the description of radionuclide solubility behaviour and speciation.

A short description of the model and main parameters is provided below, but the reader is referred to the original publications by Pitzer and/or key review works for a detailed description of the Pitzer equations and the physical theory behind [15,17–22]. The

Table 1
Solubility and hydrolysis constants of U(VI) at $I = 0$ reported in the literature for the system UO_2^{2+}–Na^+–K^+–H^+–OH^-–Cl^-–$H_2O(l)$.

Solubility reactions		$\log {}^*K^\circ_{s,0}$	References
$UO_3\cdot 2H_2O(cr) + 2H^+ \Leftrightarrow UO_2^{2+} + 3H_2O(l)$		(5.35 ± 0.13)	[5]
$1/2Na_2U_2O_7\cdot H_2O(cr) + 3H^+ \Leftrightarrow UO_2^{2+} + Na^+ + 2H_2O(l)$		(12.2 ± 0.2)	[5]
$1/2K_2U_2O_7\cdot 1.5H_2O(cr) + 3H^+ \Leftrightarrow UO_2^{2+} + K^+ + 2.25H_2O(l)$		(12.0 ± 0.2)	[6]
$1/6\ K_2U_6O_{19}\cdot 11H_2O(cr) + 7/3H^+ \Leftrightarrow UO_2^{2+} + 1/3K^+ + 3H_2O(l)$		(6.3 ± 0.1)	[6]
Hydrolysis reactions	**(xy)**	**$\log {}^*\beta^\circ_{(x,y)}$**	
$UO_2^{2+} + H_2O(l) \Leftrightarrow H^+ + UO_2OH^+$	(11)	−(5.25 ± 0.24)	[10]
$UO_2^{2+} + 2H_2O(l) \Leftrightarrow 2H^+ + UO_2(OH)_2(aq)$	(12)	−(12.15 ± 0.17)	[10]
$UO_2^{2+} + 3H_2O(l) \Leftrightarrow 3H^+ + UO_2(OH)_3^-$	(13)	−(20.7 ± 0.4)	[5]
$UO_2^{2+} + 4H_2O(l) \Leftrightarrow 4H^+ + UO_2(OH)_4^{2-}$	(14)	−(31.9 ± 0.2)	[5]
$2UO_2^{2+} + 2H_2O(l) \Leftrightarrow 2H^+ + (UO_2)_2(OH)_2^{2+}$	(22)	−(5.62 ± 0.04)	[10]
$3UO_2^{2+} + 4H_2O(l) \Leftrightarrow 4H^+ + (UO_2)_3(OH)_4^{2+}$	(34)	−(11.9 ± 0.3)	[10]
$3UO_2^{2+} + 5H_2O(l) \Leftrightarrow 5H^+ + (UO_2)_3(OH)_5^+$	(35)	−(15.55 ± 0.12)	[10]
$3UO_2^{2+} + 7H_2O(l) \Leftrightarrow 7H^+ + (UO_2)_3(OH)_7^-$	(37)	−(32.2 ± 0.8)	[10]
$4UO_2^{2+} + 7H_2O(l) \Leftrightarrow 7H^+ + (UO_2)_4(OH)_7^+$	(47)	−(21.9 ± 1.00)	[10]

model defines binary parameters $\beta^{(0)}_{MX}$, $\beta^{(1)}_{MX}$, $\beta^{(2)}_{MX}$ and $C^{(\varphi)}_{MX}$ for each anion-cation pair. $\beta^{(0)}_{MX}$ and $\beta^{(1)}_{MX}$ correspond to short-range interactions in all salt systems. $\beta^{(2)}_{MX}$ is zero except in 2–2 electrolyte systems, for which it is also highly correlated with the association constant of these ions. The contribution of $C^{(\varphi)}_{MX}$ is expected to be very small in those systems with low concentrations of reactants/products, compared to the concentration of the background electrolyte. θ_{Mc} and θ_{Xa} are asymmetrical mixing parameters for each unlike cation-cation and anion-anion pair, respectively. Ψ_{Xac} and Ψ_{Mac} correspond to the third virial coefficient representing triple interactions between ions. The interactions between ions and neutrally charged species are defined by λ_{nM} (or λ_{nX}).

In mixed electrolyte solutions with cations (c and c′) and anions (a and a′), the individual activity coefficients for a cation (M) and an anion (X) are described by Eqs. (1) and (2), respectively:

$$\ln\gamma_M = z_M^2 F + \sum_a m_a(2B_{Ma} + ZC_{Ma}) + \sum_c m_c(2\Phi_{Mc} + \sum_a m_a\psi_{Mca}) + \sum_{a<}\sum_{a'} m_a m_{a'}\psi_{Maa'} + z_M\sum_{c<}\sum_a m_c m_a C_{ca} + 2\sum_n m_n\lambda_{nM} \quad (1)$$

$$\ln\gamma_X = z_X^2 F + \sum_c m_c(2B_{cX} + ZC_{cX}) + \sum_a m_a(2\Phi_{Xa} + \sum_c m_c\psi_{cXa}) + \sum_{c<}\sum_{c'} m_c m_{c'}\psi_{cc'X} + |z_X|\sum_{c<}\sum_a m_c m_a C_{ca} + 2\sum_n m_n\lambda_{nX} \quad (2)$$

Because of the large number of binary and ternary parameters involved in the calculation of the activity coefficients with the Pitzer equations, the development of activity models based on this approach requires extensive datasets with large variations in the concentration of the background electrolyte. These requirements often affect the development of Pitzer activity models for radionuclide systems, for which available datasets are usually limited to a few background electrolyte concentrations. To overcome some of these limitations and (especially) to avoid the over-parameterization of the limited datasets, some simplifications and estimation methods were developed and previously reported [22,23]. Assuming a system in which the parameter $C^{(\varphi)}_{MX}$ is zero and mixing (θ_{Xa} or θ_{Mc}) and ternary parameters and (Ψ_{Xac} or Ψ_{Mac}) can be neglected, the general definitions of mean activity coefficient of an ion by SIT and Pitzer show very close similarities:

Mean activity coefficients in Pitzer

$$\ln\gamma_\pm = -|z_M z_X|A_\Phi\left[\frac{\sqrt{I_m}}{1+b\sqrt{I_m}} + \frac{2}{b}\ln\left(1+b\sqrt{I_m}\right)\right] + \frac{2\nu_M\nu_X}{\nu}\left(2\beta^{(0)}_{MX} + 2\beta^{(1)}_{MX}X\right)m \quad (3)$$

where

$$X = \frac{1}{\alpha^2 I_m}\left[1 - \left(1 + \alpha\sqrt{I_m} - \frac{2}{b}\alpha^2\sqrt{I_m}\right)e^{-\alpha\sqrt{I_m}}\right] \quad (4)$$

Mean activity coefficients in SIT

$$\ln\gamma_\pm = \frac{-|z_M z_X|3A_\Phi\sqrt{I_m}}{1+1.5\sqrt{I_m}} + \frac{2\nu_M\nu_X}{\nu}\varepsilon_\gamma(M,X)m \quad (5)$$

Accordingly, the SIT ion interaction coefficient can be linearly correlated to binary Pitzer parameters:

$$-\frac{|z_M z_X|A_\Phi\nu}{4\nu_M\nu_X m}\left[\frac{3\sqrt{I_m}}{1+1.5\sqrt{I_m}} - \frac{\sqrt{I_m}}{(1+b\sqrt{I_m})} - \frac{2}{b}\ln\left(1+b\sqrt{I_m}\right)\right] = \beta^{(1)}_{MX}X + \beta^{(0)}_{MX} - \frac{\varepsilon_\gamma}{2} \quad (6)$$

Table 3
Quantitative relationship between different ion combinations/charges, SIT ion interaction coefficients and Pitzer binary parameters $\beta^{(0)}_{MX}$ and $\beta^{(1)}_{MX}$, as reported in [22,23].

Ion combination	$\beta^{(0)}_{MX} - \frac{\varepsilon(M,X)\cdot\ln(10)}{2}$	$\beta^{(1)}_{MX}$
M^+, X^-	0.035	0.3
M^{2+}, X^- or M^+, X^{2-}	0.15	1.6
M^{3+}, X^- or M^+, X^{3-}	0.366	4.3
M^{4+}, X^- or M^+, X^{4-}	0.754	8.9

where

$$Y = -\frac{|z_M z_X|A_\Phi\nu}{4\nu_M\nu_X m}\left[\frac{3\sqrt{I_m}}{1+1.5\sqrt{I_m}} - \frac{\sqrt{I_m}}{(1+b\sqrt{I_m})} - \frac{2}{b}\ln\left(1+b\sqrt{I_m}\right)\right] \quad (7)$$

$$\text{Slope} = \beta^{(1)}_{MX} \qquad \text{Intercept} = \beta^{(0)}_{MX} - \frac{\varepsilon_\gamma(M,X)}{2}$$

Note that values of $\varepsilon(M,X)$ instead of $\varepsilon_\gamma(M,X)$ are generally tabulated in compilations of SIT interaction coefficients. The relationship between them is $\varepsilon(M,X) = \varepsilon_\gamma(M,X)/\ln(10)$. Calculations of X and Y values for 1-1, 1-2, 1-3 and 1-4 ion combinations reported by Grenthe and co-workers [22,23] result in a very good linearity. This provides a value of $\beta^{(1)}_{MX}$ for each charge type, as well as a linear correlation between $\beta^{(0)}_{MX}$ and $\varepsilon(M,X)$. Table 3 summarizes the quantitative relationship between SIT ion interaction coefficients and Pitzer binary parameters $\beta^{(0)}_{MX}$ and $\beta^{(1)}_{MX}$ for different ion combinations/charges. Due to the complexity of the U(VI) hydrolysis scheme and to the limited datasets available for some of the hydrolysis reactions, the Pitzer activity model developed in the present work is based on a combination of experimental data and the use of estimated parameters, as those summarized in Table 3. The validity of this approached is confirmed via the comparison of the experimental U(VI) solubility data in NaCl, KCl and $MgCl_2$ solutions over a large range of pH and ionic strength conditions with the model calculations based on the new thermodynamic Pitzer model derived in this work.

2. Experimental studies in $MgCl_2$ solutions

2.1. Chemicals

$MgCl_2{\cdot}6H_2O$ (p.a.), $Mg(OH)_2$(s) and HCl-Titrisol© were purchased from Merck. The water content in $MgCl_2{\cdot}6H_2O$ was analysed and confirmed by titration of the chloride content. All sample preparation and handling was performed in an Ar-glove box at $T = (22 \pm 2)$ °C to avoid CO_2 contamination. All solutions were prepared with purified water (Milli–Q academic, Millipore) purged for two hours with Ar before use. Detailed information on all chemicals and compounds used in the present study is provided in Table A1 as Supporting Information.

2.2. pH measurements

In salt solutions of ionic strength $I \geq 0.1$ mol·kg$_w^{-1}$, the measured pH value (pH_{exp}) is an operational value related to $[H^+]$ by $pH_m = pH_{exp} + A_m$, where A_m is a function of the background electrolyte concentration. The measurements of pH_{exp} were performed using combination pH electrodes (type ROSS, Orion) calibrated against standard pH buffers (pH = 2–9, Merck). A_m values determined as a function of $MgCl_2$ concentration are available in the literature [24]. The highest pH_m in $MgCl_2$ systems (pH_{max}) is defined by the precipitation of $Mg(OH)_2$(cr) (or $Mg_2(OH)_3Cl{\cdot}4H_2O$(cr) at $MgCl_2$ concentrations above ≈ 2 mol·kg$_w^{-1}$). These solid phases

buffer the pH_m at ≈ 9 for $[MgCl_2] \geq 0.25$ mol·dm^{-3} (the solubility of $Mg(OH)_2$(cr) in pure water buffers the pH_m at ≈ 10.3) [24].

2.3. Solubility experiments in $MgCl_2$ systems

Metaschoepite, $UO_3{\cdot}2H_2O$(cr), used for the solubility experiments was prepared and characterized as described elsewhere [5]. Solubility experiments were performed from undersaturation conditions in independent batch samples with 0.01, 0.25, 2.67 and 5.15 mol·kg$_w^{-1}$ $MgCl_2$ solutions at $4.1 \leq pH_m \leq 9.7$. pH_m values were adjusted by addition of $Mg(OH)_2$(cr) and $MgCl_2$–HCl solutions of appropriate ionic strength.

pH_m and [U] were measured at regular time intervals from 5 to 200 days. Thermodynamic equilibrium was assumed after repeated measurements with constant values of pH_m and [U]. The aqueous uranium concentration was measured by ICP–MS (inductively coupled plasma mass spectrometry) after phase separation by ultrafiltration (10 kD ≈ 2 nm, Pall Life Science). Before ICP–MS measurements, aliquots of the original samples were diluted with 2% HNO_3. Detection limits calculated as 3σ of the signal of the blank ranged between ≈ 10^{-7} and ≈ 10^{-10} mol·dm^{-3}, depending upon dilution factor/salt concentration. Note that all measurement confidences reported throughout the text are expressed as 2 times the standard deviation of the instrumental replicates. Values of [U] quantified in molar units (mol·dm^{-3}, M) were converted to molal units (mol·kg$_w^{-1}$, m) using the conversion factors reported for $MgCl_2$ solutions in the NEA–TDB [10].

After attaining equilibrium conditions, the solid phases of selected samples were characterized by X–ray diffraction (XRD). Diffractograms were collected with a Bruker AXS D8 Advance X-ray powder diffractometer at $5 \leq 2\theta \leq 60°$ with incremental steps of 0.01° to 0.04° and a measurement time of 4–30 s per step.

The aqueous speciation of uranium was also investigated by potentiometric titrations in combination with UV–vis spectroscopy. Spectroscopic measurements were conducted with a high-resolution UV–vis/NIR spectrometer Cary 5 (Varian, USA) equipment. An aliquot of the supernatant of selected solubility samples in 2.67 and 5.15 mol·kg$_w^{-1}$ $MgCl_2$ systems was taken after ultrafiltration, and the corresponding UV–vis spectra collected within $350 \leq \lambda$ [nm] ≤ 500. Samples were titrated to $pH_m \approx 2$ with HCl–$MgCl_2$ solutions of appropriate ionic strength (2.67 and 5.15 mol·kg$_w^{-1}$) with $[H^+] = 0.5$ mol·kg$_w^{-1}$. Aqueous speciation of U(VI) at this pH_m is dominated by unhydrolyzed $UO_2Cl_n^{2-n}$ species, and thus differences between added HCl and measured $[H^+]$ (pH_m) correspond to H^+ consumed in the neutralization of OH^- groups in $(UO_2)_x(OH)_y^{2x-y}$ complexes. UV–vis data of supernatant solutions were also collected after titrations to $pH_m \approx 2$.

3. Results and discussion

3.1. Solubility measurements

The U(VI) solubility data in NaCl and KCl solutions considered in this work have been reported in recent publications by Altmaier et al., 2017 [5] and Cevirim-Papaioannou et al., 2018 [6], respectively. These are not discussed again in the present paper, but will be used for comparison with the derived comprehensive thermodynamic and Pitzer activity model.

Fig. 1 shows the experimental solubility data of U(VI) determined in 0.01, 0.25, 2.67 and 5.15 mol·kg$_w^{-1}$ $MgCl_2$ systems. All data (as log [U] *vs.* pH_m) are also summarized in Tables A2 and A3 as Supporting Information. For comparison purposes, the figure includes also U(VI) solubility data determined in 5.61 mol·kg$_w^{-1}$ NaCl [5] and the solubility of $UO_3{\cdot}2H_2O$(cr) at $I = 0$ calculated using thermodynamic data in Table 1. A very significant increase in solubility (up to 3 $\log_{10}$-units) is observed with increasing $MgCl_2$ concentration from 0.01 to 5.15 mol·kg$_w^{-1}$. Similar observations were reported for the solubility of U(VI) in acidic, dilute to concentrated NaCl systems, reflecting very strong ion interaction processes between U(VI) cationic hydrolysis species and Cl^-. Indeed, the predominance of inner-sphere $UO_2Cl_x^{2-x}$ complexes (with x = 1–3) in acidic solutions with $[Cl^-] \geq 3$ mol·dm^{-3} was previously confirmed by a number of spectroscopic studies (UV–vis, EXAFS, HEXS, Raman) [25–29]. The formation of ternary complexes U(VI)–OH–Cl(aq) in weakly acidic to near-neutral pH conditions is also discussed in the literature to explain the differences observed between potentiometric studies in NaCl and $NaClO_4$ systems, although a definitive spectroscopic proof of their existence is so far missing [14,30,31].

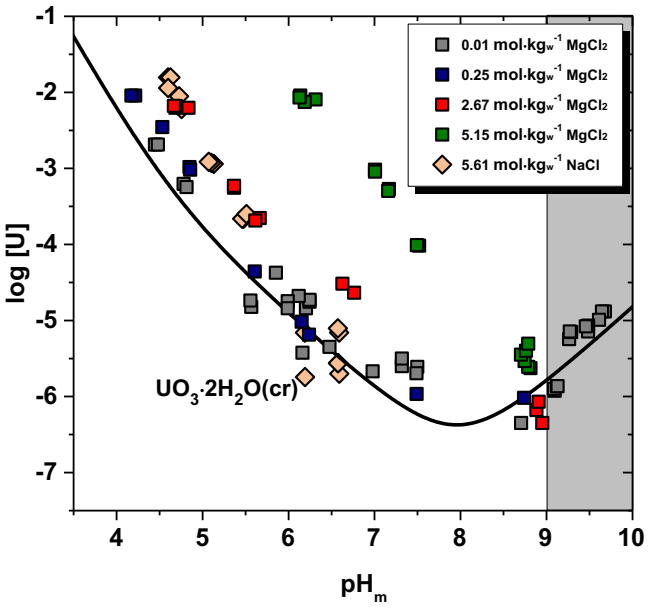

Fig. 1. Experimental solubility data of U(VI) in 0.01, 0.25, 2.67 and 5.15 mol·kg$_w^{-1}$ $MgCl_2$ solutions. Solubility data in 5.61 mol·kg$_w^{-1}$ NaCl solutions reported in [5] included for comparative purposes. Solid line corresponds to the solubility of $UO_3{\cdot}2H_2O$(cr) calculated at $I = 0$ using the thermodynamic data summarized in Table 1.

U(VI) solubility data in $MgCl_2$ solutions are limited to $pH_m \approx 9$ (pH_{max}) due to the precipitation of $Mg(OH)_2$(s) or $Mg_2(OH)_3Cl{\cdot}4H_2O$(cr), except for the 0.01 m $MgCl_2$ system for which $pH_{max} \approx 9.7$ (see [24]). In contrast to NaCl systems, no decrease in solubility is observed in any alkaline $MgCl_2$ solution within the timeframe of this study (200 days). A decrease in solubility may be caused by the ripening of an amorphous phase with (initial) small particle size, although often indicates a solid phase transformation to a less soluble compound. Hence, Altmaier and co-workers [5] reported a significant decrease in the solubility of $UO_3{\cdot}2H_2O$(cr) after equilibrating the solid for 140 days in 0.03 mol·kg$_w^{-1}$ NaCl solutions at $pH_m \geq 8.5$. A similar decrease in solubility was observed by Fanghänel and Neck [32] in weakly alkaline 0.51 and 5.61 mol·kg$_w^{-1}$ NaCl solutions. In both studies, solid phase characterization confirmed that $Na_2U_2O_7{\cdot}H_2O$(cr) was the solid phase controlling the solubility of U(VI) after completing the transformation process. The absence of such a decrease in the solubility of U(VI) in alkaline $MgCl_2$ solutions suggests that no ternary Mg–U(VI)–OH(s) solid phases formed in the conditions of our study. This hypothesis is further supported by XRD analysis of selected solubility samples in $MgCl_2$ solutions (data not shown), which confirm that the $UO_3{\cdot}2H_2O$(cr) "starting material" remains unaltered in the course of the solubility experiments.

Besides the confirmed formation of $M_2U_2O_7{\cdot}xH_2O$(cr) solid phases (with M = Na and K) in alkaline MCl systems at ambient

temperature conditions [5,6], on-going experiments at KIT–INE indicate also that $CaU_2O_7{\cdot}xH_2O$(cr) controls the solubility of U(VI) in alkaline $CaCl_2$ solutions at $pH_m \geq 7.5$. Although the NEA–TDB selected thermodynamic data for $MgUO_4$(cr), these data were determined in thermochemical studies using a highly crystalline material synthesized at $T \geq 1000$ °C [8,9]. Indeed, thermodynamic data available for the M(II)UO_4(cr) series shows the destabilization of the uranate structure with the decrease of the M(II) atomic number, with $MgUO_4$(cr) being the less stable phase and $BeUO_4$(cr) becoming unstable with respect to BeO(cr) and UO_3(cr) [8,31]:

$$UO_3(cr) + MO(cr) \Longleftrightarrow MUO_4(cr) \quad (8)$$

This phenomenon is possibly related with the small size of Be^{2+} (0.45 Å for CN = 6, 0.27 Å for CN = 4) and Mg^{2+} ions (0.72 Å for CN = 6) compared to Ca^{2+} ions (1.0 Å for CN = 6) [33]. This results in larger hydration energies and, accordingly, in a less favoured incorporation of these cations into the uranate structure. In line with this discussion and with the experimental observations collected in $MgCl_2$ solutions, we postulate that no hydrated $MgU_2O_7{\cdot}xH_2O$(cr) phases form at $T \approx 25$ °C. Consistently with this hypothesis, Lucchini and co-workers [4] proposed that $UO_3{\cdot}2H_2O$(cr) and $Na_2U_2O_7{\cdot}xH_2O$(cr) are the solid phases controlling the solubility of U(VI) in GWB ([NaCl] = 2.87 mol·dm^{-3}, [$MgCl_2$] = 0.953 mol·dm^{-3}, among other components) and ERDA-6 ([NaCl] = 4.25 mol·dm^{-3}, [$MgCl_2$] = 0.018 mol·dm^{-3}, among other components) brines.

3.2. Aqueous phase characterization

Table 4 summarizes experimentally measured [U(VI)], pH_m and corresponding OH:U ratios determined in the titration experiments in $MgCl_2$ and NaCl solutions in the present work and in Altmaier et al. [5], respectively. These values are considered in Section 3.3 for the evaluation of Pitzer interaction parameters of U(VI) hydrolysis species, in combination with additional solubility and potentiometric data obtained in the present work and reported in the literature [12–14]. Table 4 indicates also the U(VI) aqueous species prevailing (> 20%) for NaCl and $MgCl_2$ salt systems and pH_m values 4.3–6.2, as calculated with the thermodynamic and Pitzer activity models summarized in Tables 1 and 5, respectively.

UV–vis spectra of the supernatant $MgCl_2$ solutions before and after titration with HCl are shown in Fig. 2a and b, respectively. The strong absorption observed in the original solutions is in line with the predominance of U(VI) polyatomic species, as also reported by Altmaier and co-workers [5] for NaCl solutions of analogous pH_m. After titration to $pH_m \approx 2$, the absorption decreases significantly indicating that U(VI) monomeric species dominate. The significant bathochromic shift observed with increasing [Cl^-] (λ_{max} = 427 nm in 5.15 mol·kg$_w^{-1}$ $MgCl_2$, see Fig. 2b) is consistent with the formation of U(VI)–Cl complexes [25]. The spectrum of the supernatant solution in 2.67 mol·kg$_w^{-1}$ $MgCl_2$ shows similar features than those obtained in 5.6 mol·kg$_w^{-1}$ NaCl [5] but with a decreased (normalized) absorption. This is in agreement with the lower experimentally measured OH:U ratio (OH:U = 1.10 ± 0.15 in 2.67 mol·kg$_w^{-1}$ $MgCl_2$, compared to OH:U = 1.22 ± 0.15 in 5.61 mol·kg$_w^{-1}$ NaCl) in the titration experiments. The calculated model results show that U(VI) speciation in acidic, concentrated $MgCl_2$ solutions in equilibrium with $UO_3{\cdot}2H_2O$(cr) is dominated by the trimer $(UO_2)_3(OH)_4^{2+}$. Although the formation of ternary U(VI)–OH–Cl(aq) complexes is possibly expected in these conditions (*e.g.* $(UO_2)_3(OH)_4Cl^+$), the available data is insufficient for a correct parametrization of the corresponding thermodynamic properties. The explicit formation of these species

Table 4
Experimentally measured log [U], pH_m and OH:U values determined with the titration of selected supernatant solutions in NaCl [5] and $MgCl_2$ (present work) systems. Experimental values are compared to OH:U ratios calculated for each pH_m using the aqueous speciation based on the thermodynamic and Pitzer activity models summarized in Tables 1 and 5.

Matrix	log [U]	pH_m	OH:U (experimental)	OH:U (calculated)	Predominant species	Ref.
0.51 mol·kg$_w^{-1}$ NaCl	−2.6	4.3	(0.62 ± 0.07)	0.76	(10), (22)	[5]
2.64 mol·kg$_w^{-1}$ NaCl	−2.4	4.5	(0.96 ± 0.10)	0.90	(34), (10), (22)	[5]
5.61 mol·kg$_w^{-1}$ NaCl	−1.9	4.7	(1.22 ± 0.15)	1.12	(34)	[5]
2.67 mol·kg$_w^{-1}$ $MgCl_2$	−2.2	4.7	(1.10 ± 0.15)	1.09	(34)	p.w.
5.15 mol·kg$_w^{-1}$ $MgCl_2$	−2.1	6.2	(1.40 ± 0.20)	1.17	(34)	p.w.

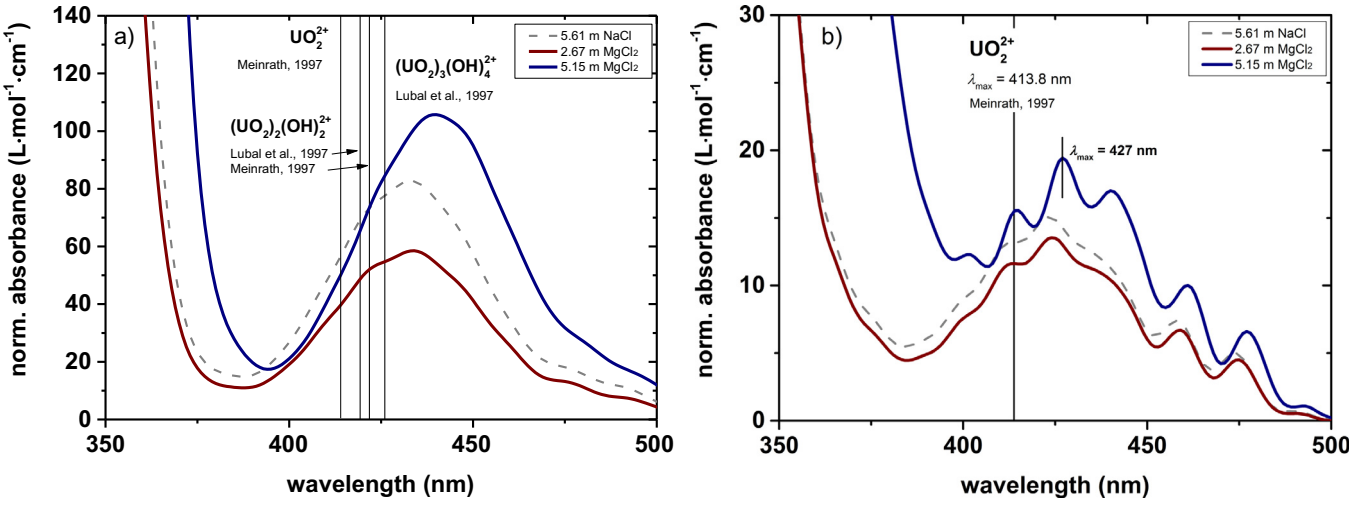

Fig. 2. Normalized UV–vis spectra of selected samples (a) before and (b) after titration to $pH_m \approx 2$ with HCl–$MgCl_2$ solutions. Concentration of U(VI) after 10 kD ultrafiltration and pH_m before titration with HCl are summarized in Table 4. Vertical lines provide the main absorption wavelengths of UO_2^{2+}, $(UO_2)_2(OH)_2^{2+}$ and $(UO_2)_3(OH)_4^{2+}$ as reported by Meinrath (1997) [34] and Lubal et al. (1997) [35].

is accordingly disregarded in chemical model derived for this system, however it is implicitly taken into account within the activity models of the hydrolysis species.

3.3. Pitzer activity model for the system UO_2^{2+}–Na^+–K^+–Mg^{2+}–H^+–OH^-–Cl^-–H_2O(l)

Chemical, thermodynamic and SIT activity models describing the solubility and hydrolysis of U(VI) in acidic to alkaline pH conditions were reviewed in the last update book of the NEA–TDB [10], and recently updated based on comprehensive experimental datasets in dilute to concentrated NaCl and KCl systems [5,6]. These data are considered in combination with the new experimental observations obtained in this work in $MgCl_2$ solutions to derive a Pitzer activity model for the system UO_2^{2+}–Na^+–K^+–Mg^{2+}–H^+–OH^-–Cl^-–H_2O(l).

3.3.1. Pitzer ion interaction coefficients for U(VI) hydrolysis species forming in acidic to near-neutral pH_m conditions

The solubility of U(VI) in the acidic pH region increases with increasing ionic strength in both NaCl and $MgCl_2$ systems. The slope of the solubility (log [U] *vs.* pH_m) varies as a function of pH_m, but also depends upon salt system and salt concentration. This reflects the complex hydrolysis scheme of U(VI), especially under acidic conditions where the greater solubility limit defined by $UO_3{\cdot}2H_2O$(cr) promotes the formation (and predominance) of a number of polyatomic species. For this reason, the same strategy considered in Altmaier et al. (2017) [5] is adopted in the present work: (i) solubility and hydrolysis constants at $I = 0$ are retained as reported in [5] and [10], respectively; (ii) binary U(VI)–Cl and ternary U(VI)–OH–Cl complexes are not explicitly considered in the chemical model, and the impact of chloride is accordingly only described by the activity model; (iii) a (Pitzer) activity model is derived based on available experimental data and considering analogies or estimation methods.

Note that there are no systematic experimental datasets as a function of ionic strength available for acidic KCl solutions. On the other hand, ion interaction processes in acidic KCl systems are dominated by the interactions between cationic U(VI) hydrolysis species and Cl^-. Accordingly, the Pitzer activity model derived in this study for U(VI) in acidic NaCl and $MgCl_2$ solutions is also expected to properly explain ion interaction processes of U(VI) in acidic KCl solutions. Experimental solubility data reported by Sandino et al. [36] in 1.0 mol·dm^{-3} KCl are compared to thermodynamic calculations using the Pitzer activity model derived in this work to confirm this hypothesis (see Section 3.4).

(11) and (47) hydrolysis species.

The monomeric species $UO_2(OH)^+$ (11) is very minor at the rather high uranium concentrations defined by $UO_3{\cdot}2H_2O$(cr) (solubility studies) or used in potentiometric studies. Drobot et al. (2016) [37] is probably the only experimental study investigating the hydrolysis of U(VI) under conditions where monomeric species are predominant (TRLFS, $[U]_{tot} = 10^{-8}$ mol·dm^{-3}). The study was performed in 1.0 mol·dm^{-3} $NaClO_4$, and thus it does not provide information on the interaction of this species with chloride. Based on systematic potentiometric titrations, De Stefano and co-workers (2002) [14] reported conditional hydrolysis constants for the (11) species in 0.1–4.5 mol·dm^{-3} NaCl solutions. However, in the conditions of their experiments ($[U]_{tot} \geq 5{\cdot}10^{-4}$ mol·dm^{-3}), the fraction of $UO_2(OH)^+$ in solution accounted for less than 2% and thus the reported log ${}^*\beta'_{(1,1)}$ are highly questionable. The tetrameric species $(UO_2)_4(OH)_7^+$ (47) has a limited predominance field under near-neutral pH conditions and high total uranium concentrations (log $[U]_{tot} > -3.5$), and there are no experimental studies reporting the variation of log ${}^*\beta'_{(4,7)}$ with chloride concentration.

For the reasons indicated above, Pitzer parameters for the (11) and (47) hydrolysis species are determined according to simplifications and estimation methods described in Section 1.2. Hence, the binary parameter C^{Φ}_{MX} and mixing parameters θ_{Xa} (or θ_{Mc}) and Ψ_{Xac} (or Ψ_{Mac}) are set to zero. $\beta^{(0)}_{(UO_2(OH)^+,\ Cl^-)}$ and $\beta^{(0)}_{((UO_2)_4(OH)_7^+,\ Cl^-)}$ are calculated based on the correlation with SIT ion interaction coefficients for 1–1 electrolytes (see Tables 2 and 3). $\beta^{(1)}_{(UO_2(OH)^+,\ Cl^-)}$ and $\beta^{(1)}_{((UO_2)_4(OH)_7^+,\ Cl^-)}$ are set to the tabulated values in Table 3. The resulting Pitzer interaction parameters for (11) and (47) species are:

$$\beta^{(0)}_{(UO_2(OH)^+,Cl^-)} = 0.15\ \mathrm{kg}\cdot\mathrm{mol}^{-1}$$
$$\beta^{(1)}_{(UO_2(OH)^+,Cl^-)} = 0.3\ \mathrm{kg}\cdot\mathrm{mol}^{-1}$$

$$\beta^{(0)}_{((UO_2)_4(OH)_7^+,Cl^-)} = 0.23\ \mathrm{kg}\cdot\mathrm{mol}^{-1}$$
$$\beta^{(1)}_{((UO_2)_4(OH)_7^+,Cl^-)} = 0.3\ \mathrm{kg}\cdot\mathrm{mol}^{-1}$$

The U(VI) hydrolysis species (11) and (47) play only a very minor role in the context of solubility studies, and thus the corresponding values of $\beta^{(0)}$ and $\beta^{(1)}$ are selected only for the sake of completeness.

(22), (34) and (35) hydrolysis species.

The polyatomic hydrolysis species $(UO_2)_2(OH)_2^{2+}$ (22), $(UO_2)_3(OH)_4^{2+}$ (34) and $(UO_2)_3(OH)_5^+$ (35) have larger predominance fields within the boundary conditions defined by solubility and potentiometric studies. For this reason, a fairly large experimental dataset dealing with these species is available in the literature, which is further complemented with the solubility, potentiometric and spectroscopic studies conducted in this work. These data can be used for an accurate determination of Pitzer ion interaction parameters of these species. The following experimental data are considered for the development of the Pitzer activity model for the (22), (34) and (35) hydrolysis species:

a) Solubility of $UO_3{\cdot}2H_2O$(cr) in 0.01–5.15 mol·kg$_w^{-1}$ $MgCl_2$ and 0.03–5.61 mol·kg$_w^{-1}$ NaCl, as determined in the present work and reported in Altmaier et al., 2017 [5], respectively. Both studies provide values of pH_m and log $[U]_{tot}$, where $[U]_{tot}$ can be calculated according with equation (9):

$$[U]_{tot} = \left[UO_2^{2+}\right] + \sum x\left[(UO_2)_x(OH)_y^{2x-y}\right] = {}^*K'_{s,0*}\left[H^+\right]^2 + \sum x\left({}^*K'_{s,0*}\left[H^+\right]^2\right)^x {}^*\beta'_{(x,y)*}\left[H^+\right]^{-y} \quad (9)$$

b) Conditional equilibrium constants determined in potentiometric studies for the formation of (22), (34) and (35) species ([12–14], see reactions (10)–(12)). Data reported in [12–14] are available for a wide range of NaCl concentrations: 0.1–4.5 mol·dm^{-3} (or 0.1–4.98 mol·kg$_w^{-1}$).

$$2\,UO_2^{2+} + 2\,H_2O(l) \Longleftrightarrow (UO_2)_2(OH)_2^{2+} + 2\,H^+ \quad (10)$$

$$3\,UO_2^{2+} + 4\,H_2O(l) \Longleftrightarrow (UO_2)_3(OH)_4^{2+} + 4\,H^+ \quad (11)$$

$$3\,UO_2^{2+} + 5\,H_2O(l) \Longleftrightarrow (UO_2)_3(OH)_5^{+} + 5\,H^+ \quad (12)$$

c) Titration experiments performed in the present study ($MgCl_2$ systems) and in [5] (NaCl systems), which provide experimental OH:U ratios at a given pH_m and salt concentration (Table 4).

The determination of the Pitzer interaction parameters for the (22), (34) and (35) species was performed by minimizing the squared root of the difference between calculated and experimental data in a), b) and c). Because of the large and diverse dataset, a weighting scheme was applied in the minimization routine: (a) a weight of 0.5 was given to solubility studies, (b) a weight of 0.4 to potentiometric studies, and (c) a weight of 0.1 to titration experiments. This weighting scheme reflects the size of each dataset (a–c), but also the greater relevance given in this work to the need of accurately describing solubility phenomena.

Equilibrium constants at $I = 0$ for U(VI) hydrolysis species ($\log {}^{*}\beta^{\circ}_{(x,y)}$) and $UO_3{\cdot}2H_2O$(cr) solubility ($\log {}^{*}K^{\circ}_{s,0}$) were kept constant and taken as summarized in Table 1. Considering the complexity of the system and for the sake of simplicity, the minimization routine targeted the optimization of $\beta^{(0)}$ and $\beta^{(1)}$ for the (22), (34) and (35) species. Mixing (θ_{Mc} (or θ_{Xa}) and ternary parameters (Ψ_{Xac} (or Ψ_{Mac})) for asymmetrical mixing (2-1 interactions) were originally set to 0. This approach provided satisfactory results for (22) and (35) species, but not for (34) in the NaCl system. The ternary parameter for asymmetrical mixing $\Psi_{(34,\ Na^+,\ Cl^-)}$ was accordingly considered in the final fit of this species. $\beta^{(2)}$ and C^{Φ}_{MX} were disregarded in all cases for the reasons given in Section 1.2. The values of $\log\gamma_{H^+}$ and a_w are calculated considering Pitzer interaction parameters reported by Harvie et al. [38]. $\log\gamma_{UO_2^{2+}}$ is calculated with well-known binary Pitzer parameters of UO_2^{2+} from Pitzer et al. (1991) [15] and ternary parameters derived by Altmaier et al. (2009) [39]. $\log\gamma_{UO_2OH^+}$, $\log\gamma_{(UO_2)_4OH_7^+}$, $\log\gamma_{UO_2(OH)_3^-}$, $\log\gamma_{(UO_2)_3OH_7^-}$ and $\log\gamma_{UO_2(OH)_4^{2-}}$ are calculated with the Pitzer interaction parameters derived in the present study (Table 5) and kept constant in the optimization of Pitzer parameters for (22), (34) and (35) species. The minimization routine was applied simultaneously to datasets a), b) and c) considering the weighting factors, assumptions and boundary conditions described above. This resulted in the following Pitzer parameters for $(UO_2)_2(OH)_2^{2+}$, $(UO_2)_3(OH)_4^{2+}$ and $(UO_2)_3(OH)_5^{+}$ species:

$$\beta^{(0)}_{((UO_2)_2(OH)_2^{2+},Cl^-)} = 0.389\ \mathrm{kg\cdot mol^{-1}}$$
$$\beta^{(1)}_{((UO_2)_2(OH)_2^{2+},Cl^-)} = 2.259\ \mathrm{kg\cdot mol^{-1}}$$

$$\theta_{((UO_2)_2(OH)_2^{2+},Na^+)} = 0$$
$$\Psi_{((UO_2)_2(OH)_2^{2+},Na^+,Cl^-)} = 0$$

$$\beta^{(0)}_{((UO_2)_3(OH)_4^{2+},Cl^-)} = 0.08\ \mathrm{kg\cdot mol^{-1}}$$
$$\beta^{(1)}_{((UO_2)_3(OH)_4^{2+},Cl^-)} = 1.4\ \mathrm{kg\cdot mol^{-1}}$$

$$\theta_{((UO_2)_3(OH)_4^{2+},Na^+)} = 0$$
$$\Psi_{((UO_2)_3(OH)_4^{2+},Na^+,Cl^-)} = 0.02$$

$$\beta^{(0)}_{((UO_2)_3(OH)_5^{+},Cl^-)} = 0.146\ \mathrm{kg\cdot mol^{-1}}$$
$$\beta^{(1)}_{((UO_2)_3(OH)_5^{+},Cl^-)} = 0.6\ \mathrm{kg\cdot mol^{-1}}$$

$$\theta_{((UO_2)_3(OH)_5^{+},Na^+)} = 0$$
$$\Psi_{((UO_2)_3(OH)_5^{+},Na^+,Cl^-)} = 0$$

Values of $\beta^{(0)}$, $\beta^{(1)}$ and Ψ_{Mac} parameters qualitatively agree with the general trends expected for Pitzer parameters [15]. Experimental solubility data, conditional hydrolysis constants reported from potentiometric studies, and OH:U ratios determined in titration experiments are compared in Section 3.4, Fig. 3 and Table 4,

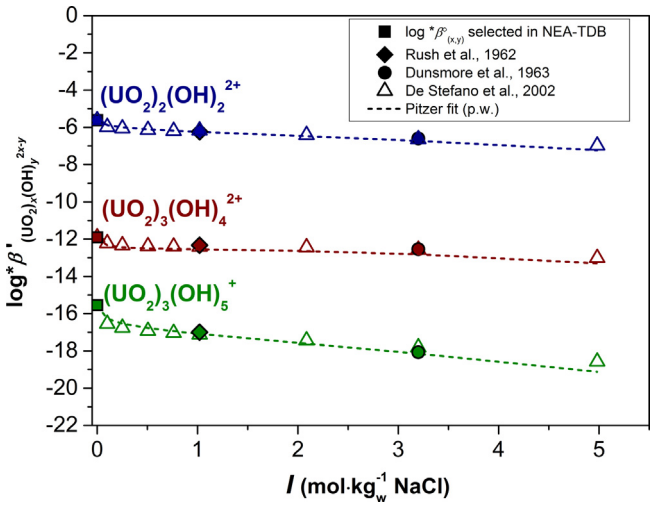

Fig. 3. Conditional equilibrium constants, $\log {}^{*}\beta'_{(x,y)}$, for the formation of the cationic hydrolysis species (22), (34) and (35) as a function of NaCl concentration: experimental values (symbols) reported in [12–14] and calculated functions (dashed lines) using equilibrium constants summarized in Table 1 and Pitzer interaction coefficients derived in the present study.

respectively, with model calculation performed with the Pitzer parameters derived in this work and equilibrium constants summarized in Table 1.

Fig. 3 shows the very good agreement between model calculations and experimental potentiometric data in dilute to concentrated NaCl solutions. Somewhat larger deviations are observed for the (35) species in 4.98 $\mathrm{mol\cdot kg_w^{-1}}$ NaCl. Undersaturation solubility experiments are considered to provide a more accurate representation of long-term equilibrium conditions, which is also reflected in the greater weight given in this work to this type of studies. Table 4 shows the comparison between OH:U ratios determined in this work by potentiometric titration experiments and the calculated values using equilibrium constants summarized in Table 1 and Pitzer interaction coefficients derived in the present study. The comparison shows the good agreement obtained for both NaCl and $MgCl_2$ systems.

3.3.2. Pitzer ion interaction coefficients for U(VI) hydrolysis species forming in alkaline to hyper-alkaline pH_m conditions

The solubility of U(VI) in alkaline MCl solutions (with M = Na and K) is dominated by the equilibrium between $M_2U_2O_7{\cdot}xH_2O$(cr) and the aqueous species $UO_2(OH)_3^-$ and $UO_2(OH)_4^{2-}$. Equilibrium reactions can be accordingly defined as:

$$0.5\,M_2U_2O_7\cdot xH_2O(cr) + (1.5-0.5x)H_2O(l) \Longleftrightarrow UO_2(OH)_3^- + M^+ \quad (13)$$

$$0.5\,M_2U_2O_7\cdot xH_2O(cr) + (2.5-0.5x)H_2O(l) \Longleftrightarrow UO_2(OH)_4^{2-} + M^+ + H^+ \quad (14)$$

with

$$\log K'_{s,(1,3)} = \log\left[UO_2(OH)_3^-\right] + \log[M^+] \quad (15)$$

$$\log^{*}K^{o}_{s,(1,3)} = \log^{*}K'_{s,(1,3)} + \log\gamma_{UO_2(OH)_3^-} + \log\gamma_{M^+} - (1.5-x)\log a_w \quad (16)$$

and

$$\log^{*}K'_{s,(1,4)} = \log\left[UO_2(OH)_4^{2-}\right] + \log[M^+] + \log[H^+] \quad (17)$$

$$\log^{*}K^{o}_{s,(1,4)} = \log^{*}K'_{s,(1,4)} + \log\gamma_{UO_2(OH)_4^{2-}} + \log\gamma_{M^+} + \log\gamma_{H^+} - (2.5-x)\log a_w \quad (18)$$

Conditional solubility constants reported for reactions (13) and (14) in NaCl [5] and KCl [6] systems are evaluated according to equations (16) and (18), where activity coefficients are calculated using the Pitzer formulism. The values of log $^*K°_{s,(1,3)}$ and log $^*K°_{s,(1,4)}$ are kept constant as calculated from thermodynamic data summarized in Table 1, and thus the Pitzer interaction coefficients required to calculate log $\gamma_{UO_2(OH)_3^-}$ and log $\gamma_{UO_2(OH)_4^{2-}}$ remain as the only unknown parameters. The values of $\beta^{(2)}$, $C^{(\Phi)}$ and the mixing parameters θ and Ψ are set to zero for both species. Under these assumptions and boundary conditions, $\beta^{(0)}$ and $\beta^{(1)}$ are optimized by minimizing the difference between calculated and experimental log $^*K'_{s,(1,4)}$ (NaCl and KCl systems) and log $^*K'_{s,(1,3)}$ (only NaCl system). The resulting Pitzer parameters are summarized below, where the values of $\beta^{(0)}_{(UO_2(OH)_3^-,K^+)}$ and $\beta^{(1)}_{(UO_2(OH)_3^-,K^+)}$ are taken in analogy to the NaCl system:

$$\beta^{(0)}_{(UO_2(OH)_3^-,Na^+)} = -0.26\,kg\cdot mol^{-1}$$
$$\beta^{(1)}_{(UO_2(OH)_3^-,Na^+)} = 0.34\,kg\cdot mol^{-1}$$

$$\beta^{(0)}_{(UO_2(OH)_4^{2-},Na^+)} = 0.065\,kg\cdot mol^{-1}$$
$$\beta^{(1)}_{(UO_2(OH)_4^{2-},Na^+)} = 1.98\,kg\cdot mol^{-1}$$

$$\beta^{(0)}_{(UO_2(OH)_3^-,K^+)} = -0.26\,kg\cdot mol^{-1}$$
$$\beta^{(1)}_{(UO_2(OH)_3^-,K^+)} = 0.34\,kg\cdot mol^{-1}$$

$$\beta^{(0)}_{(UO_2(OH)_4^{2-},K^+)} = 0.13\,kg\cdot mol^{-1}$$
$$\beta^{(1)}_{(UO_2(OH)_4^{2-},K^+)} = 2.05\,kg\cdot mol^{-1}$$

Fig. 4 compares conditional solubility constants log $^*K'_{s,(1,3)}$ and log$^*K'_{s,(1,4)}$ determined experimentally in [5] and [6] with thermodynamic calculations using equilibrium constants at $I = 0$ summarized in Table 1 and Pitzer interaction parameters derived in the present work. The figure highlights the close analogies existing between alkaline NaCl and KCl systems, and shows the excellent agreement between experimental and calculated solubility constants (Fig 4).

Due to the limitations in pH_m imposed by $MgCl_2$ (with $pH_{max} \approx 9$ at $[MgCl_2] \geq 0.25\ mol\cdot dm^{-3}$), U(VI) solubility data determined in this background electrolyte is insufficient to derive (Pitzer) interaction parameters for the hydrolysis species $UO_2(OH)_3^-$ (13) and $UO_2(OH)_4^{2-}$ (14) prevailing in alkaline to hyperalkaline pH_m conditions. Therefore, Pitzer parameters for the interaction of $UO_2(OH)_3^-$ with Mg^{2+} are estimated based on charge analogies. Pitzer parameters for the interaction of $UO_2(OH)_4^{2-}$ with Mg^{2+} are not required, as this species is only relevant above $pH_m \approx 11$.

In their systematic potentiometric study, De Stefano and co-workers (2002) determined conditional formation constants for the trimeric hydrolysis species $(UO_2)_3(OH)_7^-$ (37) in dilute to concentrated NaCl and $NaNO_3$ solutions. This species prevails within $6.5 \leq pH_m \leq 7.5$ (depending upon background electrolyte concentration), where $UO_3{\cdot}2H_2O$(cr) and $Na_2U_2O_7{\cdot}H_2O$(cr) impose

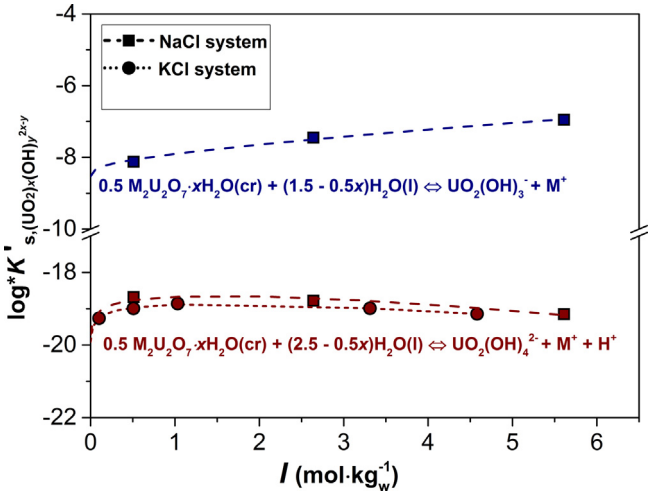

Fig. 4. Conditional solubility constants log $^*K'_{s,(x,y)}$ for equilibrium reactions (13) and (14) as a function of NaCl and KCl concentrations (in molal units): experimental values (symbols) and calculated functions (dashed line: NaCl, dotted line: KCl) based on equilibrium constants at $I = 0$ reported in Table 1 and Pitzer interaction coefficients derived in this work.

Table 5
Pitzer interaction parameters determined in this work for U(VI) hydrolysis species, and reported in the literature for UO_2^{2+} [15,39].

U(VI) species		Pitzer binary parameters				
i	*j*	$\beta^{(0)}$	$\beta^{(1)}$	$\beta^{(2)}$	C^{φ}	References
UO_2^{2+}	Cl^-	0.4274	1.644	0	−0.0368	[15]
UO_2OH^+	Cl^-	0.15	0.3	0	0	(p.w.)
$(UO_2)_2(OH)_2^{2+}$	Cl^-	0.389	2.259	0	0	(p.w.)
$(UO_2)_3(OH)_4^{2+}$	Cl^-	0.08	1.4	0	0	(p.w.)
$(UO_2)_3(OH)_5^+$	Cl^-	0.146	0.6	0	0	(p.w.)
$(UO_2)_4(OH)_7^+$	Cl^-	0.23	0.3	0	0	(p.w.)
$UO_2(OH)_3^-$	Na^+	−0.26	0.34	0	0	(p.w.)
	K^+	−0.26	0.34	0	0	(p.w.)[a]
	Mg^{2+}	0.20	1.6	0	0	(p.w.)
$UO_2(OH)_4^{2-}$	Na^+	0.06	1.98	0	0	(p.w.)
	K^+	0.13	2.05	0	0	(p.w.)
$(UO_2)_3(OH)_7^-$	Na^+	−0.26	0.34	0	0	(p.w.)[b]
	K^+	−0.26	0.34	0	0	(p.w.)[b]
	Mg^{2+}	0.20	1.6	0	0	(p.w.)[b]
$UO_2(OH)_2$(aq)	Na^+, K^+, Mg^{2+},Cl^-	0	0	0	0	(p.w.)
i	*j*	*i'*	Pitzer ternary parameters			
UO_2^{2+}	Cl^-	Na^+	$\theta_{ii'}$ = 0.03	$\Psi_{iji'}$ = −0.01		[39]
	Cl^-	Mg^{2+}	$\theta_{ii'}$ = 0.08	$\Psi_{iji'}$ = −0.072		[39]
$(UO_2)_3(OH)_4^{2+}$	Cl^-	Na^+		$\Psi_{iji'}$ = 0.02		(p.w.)

[a]Set equal to the Pitzer parameters of the same species with Na^+, b. set equal to the interaction parameter of $UO_2(OH)_3^-$ with the same cation (Na^+, K^+ or Mg^{2+}).

solubility limits well below 10^{-5} mol·dm^{-3}. Accordingly, thermodynamic data reported for this species by De Stefano and coworkers are not considered reliable because of the large oversaturated conditions required in their potentiometric study (with [U] ≥ $5{\cdot}10^{-4}$ mol·dm^{-3}). Due to the very limited solubility data available in this pH_m-region, Pitzer interaction parameters for this species are set equal to those of the $UO_2(OH)_3^-$ (13) species.

3.4. Summary of Pitzer parameters derived in the present study for the UO_2^{2+}–Na^+–K^+–Mg^{2+}–H^+–OH^-–Cl^-–H_2O(l) system and comparison with experimental solubility data

Table 5 summarizes the Pitzer interaction parameters derived in this work for U(VI) hydrolysis species in NaCl, KCl and $MgCl_2$ systems. Figs. 5–7 show all experimental solubility data determined in the present work and reported in the literature [5,6,36] in dilute to concentrated NaCl, KCl and $MgCl_2$, respectively, in comparison with the thermodynamic calculations performed using the SIT and Pitzer activity models selected in the present study (see Tables 1, 2 and 5). Model calculations are in excellent agreement with experimental results for all evaluated systems. Thermodynamic calculations in Figs. 5–7 show also a very good agreement between SIT and Pitzer approaches, further confirming the quality and robustness of the activity models derived. The present work provides the most comprehensive Pitzer activity model for U(VI) in dilute to concentrated chloride systems covering acidic to hyperalkaline pH conditions, which allows accurate solubility calculations under a variety of geochemical conditions of relevance in the context of nuclear waste disposal.

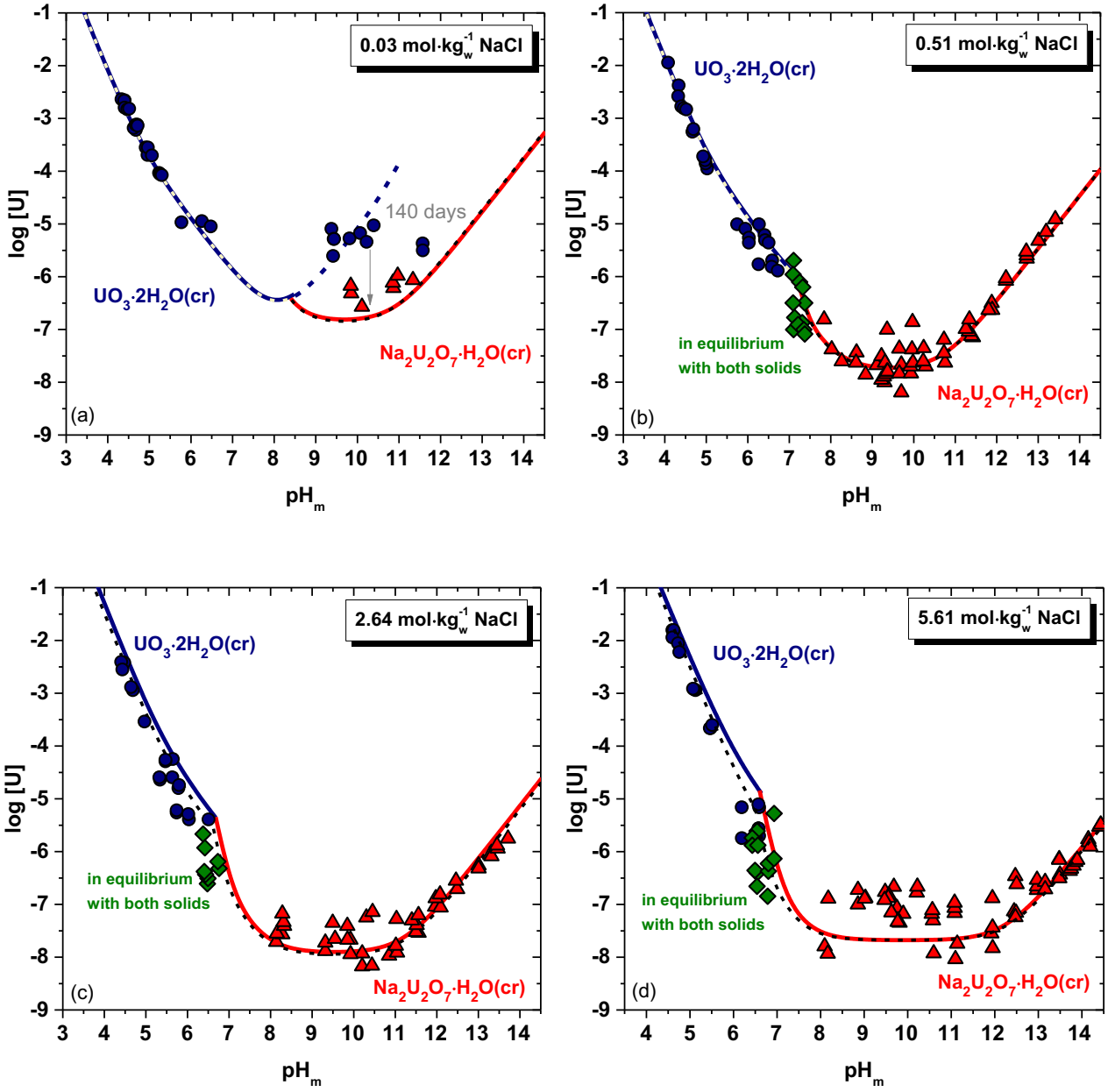

Fig. 5. Experimental solubility data of U(VI) in (a) 0.03, (b) 0.51, (c) 2.64 and (d) 5.61 mol·kg$_w^{-1}$ NaCl solutions reported in Altmaier et al., 2017 [5]. Blue symbols: samples equilibrated with $UO_3{\cdot}2H_2O$(cr); red symbols: samples equilibrated with $Na_2U_2O_7{\cdot}H_2O$(cr); green symbols: samples equilibrated with both $UO_3{\cdot}2H_2O$(cr) and $Na_2U_2O_7{\cdot}H_2O$(cr). Solid and dashed lines are the calculated solubility with the thermodynamic data and the selected Pitzer and SIT activity models, respectively (see Tables 1, 2 and 5). (For interpretation of the references to colour in this figure legend, the reader is referred to the web version of this article.)

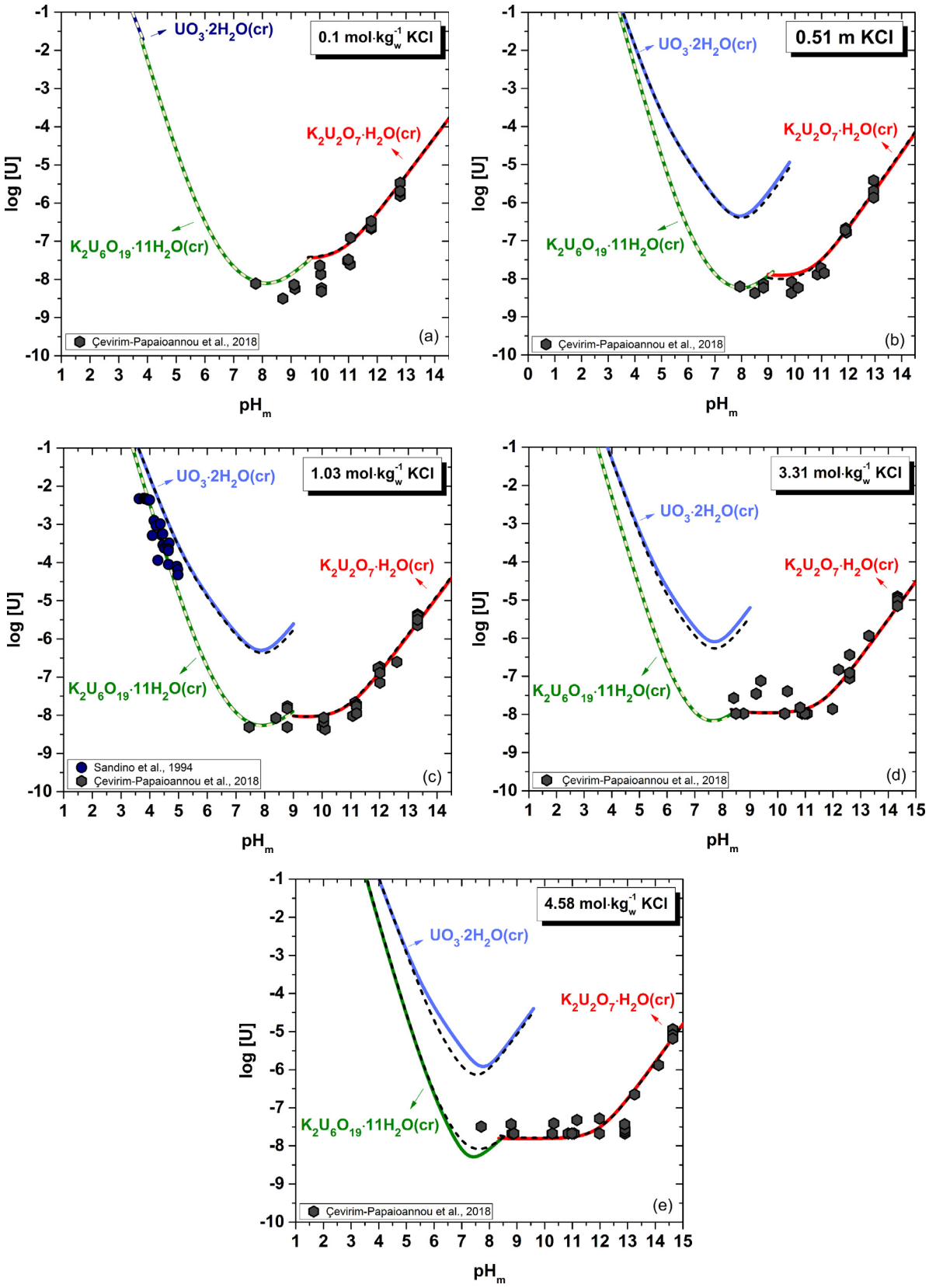

Fig. 6. Experimental solubility data of U(VI) in (a) 0.1, (b) 0.51, (c) 1.03, (d) 3.31 and (e) 4.58 mol·kg$_w^{-1}$ KCl solutions reported in Cevirim-Papaioannou et al., 2018 [6] and Sandino et al., 1994 [36]. Solid and dashed lines are the calculated solubility with the thermodynamic data and the selected Pitzer and SIT activity models, respectively (see Tables 1, 2 and 5).

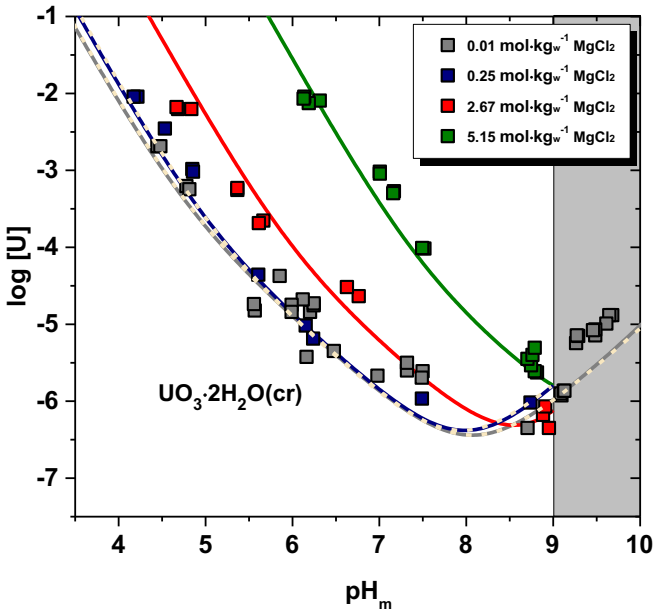

Fig. 7. Experimental solubility data of U(VI) in 0.01, 0.26, 2.67 and 5.15 mol·kg$_w^{-1}$ $MgCl_2$ solutions. Solid and dashed lines are the calculated solubility with the thermodynamic data and the selected Pitzer and SIT activity models, respectively (see Tables 1, 2 and 5). Note that only the Pitzer activity model is used for the systems at $I \geq 8$ mol·kg$_w^{-1}$. SIT coefficients for $\varepsilon(UO_2(OH)_3^-, Mg^{2+})$ = 0.04 ± 0.1 kg·mol^{-1} and $\varepsilon((UO_2)_3(OH)_7^-, Mg^{2+})$ = 0.04 ± 0.1 kg·mol^{-1} are calculated based on the Pitzer parameter $\beta^{(0)}$ of the same species according to Table 3.

4. Conclusions

This study provides the most comprehensive Pitzer activity model available to date for the system UO_2^{2+}–Na^+–K^+–Mg^{2+}–H^+–OH^-–Cl^-–H_2O(l). The new model is based on experimental solubility data determined in this work for dilute to concentrated $MgCl_2$ system, in combination with previous experimental results reported in the literature for NaCl and KCl systems.

Metaschoepite (UO_3·2H_2O(cr)) is the only solid phase controlling the solubility of U(VI) in dilute to concentrated $MgCl_2$ solutions within the pH$_m$-range investigated (4.1–9.7). In contrast to alkaline NaCl, KCl and $CaCl_2$ systems, no transformation of UO_3·2H_2O(cr) into a Mg–U(VI)–OH(s) solid phase was observed at ambient temperature conditions (22 ± 2 °C) within the timeframe of this study (≤ 200 days). Strong ion interaction processes are responsible for the significant increase in the solubility (up to 3 log$_{10}$-units) observed in concentrated $MgCl_2$, compared to dilute systems.

Uranium(VI) solubility data determined in this work in $MgCl_2$ systems, together with previously reported solubility and potentiometric studies in dilute to concentrated NaCl and KCl have been considered to derive a comprehensive Pitzer activity model for the system UO_2^{2+}–Na^+–K^+–Mg^{2+}–H^+–OH^-–Cl^-–H_2O(l). This activity model builds on the chemical and thermodynamic models recently updated by Altmaier and co-workers [5] for the solubility and hydrolysis of U(VI). The resulting thermodynamic dataset is able to satisfactorily explain all experimental observations in dilute to concentrated NaCl, KCl and $MgCl_2$ solutions. The reported thermodynamic and activity models allow robust and accurate solubility calculations that can be used in source term estimations of repositories for nuclear waste disposal. For the first time, the Pitzer activity model derived in this work can be reliably applied to very concentrated brines and pH$_m$ conditions as those eventually expected in certain disposal concepts in salt-rock formations.

Acknowledgments

This study was funded by the German Ministry of Economic Affairs and Energy (BMWi) within the framework of the EDUKEM project under the contract number 02E11334. The KIT-INE analytical staff involved in the studies are acknowledged for their contributions.

Appendix A. Supplementary data

Supplementary data to this article can be found online at https://doi.org/10.1016/j.jct.2018.10.019.

References

[1] H.F.W. Taylor, Cement Chemistry, second ed., Thomas Telford, London, 1997.
[2] E. Wieland, L.R. Van Loon, Cementitious Near-Field Sorption Data Base for Performance Assessment of an ILW Repository in Opalinus Clay, Nuclear Energy and Safety Research Department Laboratory for Waste Management, 2006.
[3] B. Kienzler et al., Geochemically based safety assessment, J. Nucl. Sci. Technol. 44 (2007) 470–476.
[4] J.F. Lucchini et al., Uranium(VI) solubility in carbonate-free WIPP brine, Radiochim. Acta 101 (6) (2013) 391–398.
[5] M. Altmaier et al., Solubility of U(VI) in chloride solutions. I. The stable oxides/hydroxides in NaCl systems, solubility products, hydrolysis constants and SIT coefficients, J. Chem. Thermodyn. 114 (2017) 2–13.
[6] N. Cevirim-Papaioannou et al., Solubility of U(VI) in chloride solutions. II. The stable oxides/hydroxides in alkaline KCl solutions: thermodynamic description and relevance in cementitious systems, Appl. Geochem. 98 (2018) 237–246.
[7] Altmaier, M., et al. Solubility of U(VI) and formation of CaU_2O_7.3H_2O(cr) in alkaline $CaCl_2$ solutions,. in: International Conference on Chemistry and Migration Behaviour of Actinides and Fission Products in the Geosphere, 2005. Avignon, France.
[8] P.A.G. O'hare et al., Thermochemistry of uranium-compounds.9. Standard enthalpy of formation and high-temperature thermodynamic functions of magnesium uranate ($MgUO_4$) – comment on nonexistence of beryllium uranate, J. Chem. Thermodyn. 9 (10) (1977) 963–972.
[9] E.H.P. Cordfunke, P.A.G. Ohare, The chemical thermodynamics of actinide elements and compounds: Part 3. Miscellaneous actinide compounds, Int. Atomic Energy Agency (1978) 83.
[10] R. Guillaumont (Ed.), Update on the Chemical Thermodynamics of Uranium, Neptunium, Plutonium, Americium and Technetium, Elsevier, North-Holland, Amsterdam, 2003, vol. 5.
[11] R. Vochten, L.V. Haverbeke, R. Sobry, Transformation of schoepite into uranyl oxide hydrates of the bivalent cations Mg^{2+}, Mn^{2+} and Ni^{2+}, J. Mater. Chem. 1 (1991) 637–642.
[12] R.M. Rush, J.S. Johnson, K.A. Kraus, Hydrolysis of uranium(VI) – ultracentrifugation and acidity measurements in chloride solutions, Inorganic Chem. 1 (2) (1962) 378.
[13] H.S. Dunsmore, L.G. Sillen, Studies on hydrolysis of metal ions. 47. Uranyl ion in 3 M (Na)Cl medium, Acta Chem. Scand. 17 (10) (1963) 2657–3000.
[14] C. De Stefano et al., Dependence on ionic strength of the hydrolysis constants for dioxouranium(VI) in NaCl(aq) and $NaNO_3$(aq), at pH 6 and t = 25 °C, J. Chem. Eng. Data 47 (3) (2002) 533–538.
[15] Pitzer, K.S., (Ed.), Activity coefficients in electrolyte solutions. 1991: Boca Raton, FL (Chapter 3).
[16] L. Ciavatta, The specific interaction theory in evaluating ionic equilibria, Anal. Chim. 70 (11–1) (1980) 551–567.
[17] K.S. Pitzer, Thermodynamics of electrolytes. I. Theoretical basis and general equations, J. Phys. Chem. 77 (1972) 268–277.
[18] K.S. Pitzer, G. Mayorga, Thermodynamics of electrolytes. II. Activity and osmotic coefficients for strong electrolytes with one or both ions univalent, J. Phys. Chem. 77 (1973) 2300–2307.
[19] K.S. Pitzer, Thermodynamics of electrolytes. III. Activity and osmotic coefficients for 2–2 electrolytes, J. Solution Chem. 3 (1974) 539–546.
[20] K.S. Pitzer, J. Kim, Thermodynamics of electrolytes. IV. Activity and osmotic coefficients for mixed electrolytes, J. Am. Chem. Soc. 96 (1974) 5701–5707.
[21] K.S. Pitzer, Thermodynamics of electrolytes. V. Effects of higher-order electrostatic terms, J. Solution Chem. 4 (1975) 249–265.
[22] I. Grenthe, I. Puigdomenech (Eds.), Modelling in Aquatic Chemistry. OECD Nuclear Energy Agency, Elsevier, Paris, 1997.
[23] A. Plyasunov, T. Fanghänel, I. Grenthe, Estimation of the Pitzer equation parameters for aqueous complexes. A case study for uranium at 298.15 K and 1 atm, Acta Chem. Scand. 52 (3) (1998) 250–260.
[24] M. Altmaier et al., Solid-liquid equilibria of $Mg(OH)_2$(cr) and $Mg_2(OH)_3Cl.4H_2O$ (cr) in the system Mg-Na-H-OH-O-Cl-H_2O at 25°C, Geochim. Cosmochim. Acta 67 (19) (2003) 3595–3601.
[25] W. Runde et al., Spectroscopic investigation of actinide speciation in concnetrated chloride solution Mat, Res. Soc. Symp. Proc. 465 (1997) 693–703.

[26] P.G. Allen et al., Investigation of aquo and chloro complexes of UO_2^{2+}, NpO_2^{+}, Np^{4+}, and Pu^{3+} by X-ray absorption fine structure spectroscopy, Inorg. Chem. 36 (1997) 4676–4683.
[27] C. Hennig et al., Comparative EXAFS investigation of uranium(VI) and -(IV) aquo chloro complexes in solution using a newly developed spectroelectrochemical cell, Inorg. Chem. 44 (2005) 6655–6661.
[28] L. Soderholm, S. Skanthakumar, R.E. Wilson, Structural correspondence between uranyl chloride complexes in solution and their stability constants, J. Phys. Chem. 115 (2011) 4959–4967.
[29] M. Dargent et al., Experimental study of uranyl(VI) chloride complex formation in acidic LiCl aqueous solutions under hydrothermal conditions (T = 21 °C – 350 °C, Psat) using Raman spectroscopy, Eur. J. Mineral. 25 (2013) 768–775.
[30] C.F. Baes, R.E. Mesmer (Eds.), Hydrolysis of Cations, John Wiley & Sons, 1976.
[31] I. Grenthe (Ed.), Chemical thermodynamics of uranium, vol. 1, Elsevier, Issy-les-Moulineaux (France), 1992.
[32] T. Fanghänel, V. Neck, Aquatic chemistry and solubility phenomena of actinide oxides/hydroxides, Pure Appl. Chem. 74 (10) (2002) 1895–1907.
[33] R.D. Shannon, Revised effective ionic-radii and systematic studies of interatomic distances in halides and chalcogenides, Acta Crystallogr. Section A 32 (Sep1) (1976) 751–767.
[34] G. Meinrath, Uranium(VI) speciation by spectroscopy, J. Radioanal. Nucl. Chem. 224 (1–2) (1997) 119–126.
[35] P. Lubal, J. Havel, Spectrophotometric and potentiometric study of uranyl hydrolysis in perchlorate medium. Is derivative spectrophotometry suitable for search of the chemical model?, Chem Pap. 51 (4) (1997) 213–220.
[36] M.C.A. Sandino, B. Grambow, Solubility equilibria in the U(VI)-Ca-K-Cl-H_2O system – transformation of schoepite into becquerelite and compreignacite, Radiochim. Acta 66–7 (1994) 37–43.
[37] B. Drobot et al., Speciation studies of metals in trace concentrations: the mononuclear uranyl(VI) hydroxo complexes, Anal. Chem. 88 (7) (2016) 3548–3555.
[38] C.E. Harvie, N. Moller, J.H. Weare, The prediction of mineral solubilities in natural-waters – the Na-K-Mg-Ca-H-Cl-SO_4-OH-HCO_3-CO_3-CO_2-H_2O system to high ionic strengths at 25°C, Geochim. Cosmochim. Acta 48 (4) (1984) 723–751.
[39] M. Altmaier, V. Neck, J. Lützenkirchen, SIT and Pitzer model for the UO_2^{2+} ion in NaCl, $MgCl_2$ and $CaCl_2$ solutions applied to trace activity coefficients determined by solvent extraction by TBP, in: International Conference on Chemistry and Migration Behaviour of Actinides and Fission Products in the Geosphere, 2009, Washington, United States.

JCT 2018-825